IX ECCOMAS Thematic Conference on Smart Structures and Materials
SMART 2019
A. Benjeddou, N. Mechbal and J.F. Deü (Eds)

THE USE OF DIFFERENT MODAL QUANTITIES FOR DAMAGE IDENTIFICATION

FABRIZIO VESTRONI*, JACOPO CIAMBELLA* AND ANNAMARIA PAU†

*Department of Structural and Geotechnical Engineering
Sapienza University of Rome, via Eudossiana 18, 00184 Rome, Italy
email: vestroni@uniroma1.it

†Department of Structural and Geotechnical Engineering
Sapienza University of Rome, via A. Gramsci 53, 00197 Rome, Italy

Key words: Damage Detection, Inverse Problem, Modal Curvatures, Modal Frequencies

Abstract. The problem of identifying small damages in beam-like structures is studied by defining a suitable inverse problem with different modal quantities including frequencies, mode shapes and modal curvatures. With the aim of making a critical analysis of the different approach followed in the literature, we study a prototype problem of a free-free beam with single and multiple damages. The attention is mainly devoted to modal curvatures. It is shown that by making use of a perturbative solution of the equation of motion of a damaged beam, it is possible to obtain a closed form relationship between the modal curvature differences due to damage and the damage distribution itself. This information is added to the contributions of other modal quantities, frequencies and mode shapes, to improve the inverse problem of damage identification and to eliminate possible redundant solutions. On the other side, the variations of the curvature due to damage is concentrated at damage location and this circumstance can lead to difficulties in its detection. The results of the proposed approach are validated by using the results of an experimental campaign carried out by the authors.

1 INTRODUCTION

Vibration-based damage identification techniques have recently been the subject of much research, with particular emphasis on natural frequencies [1, 2]. As a global structural property, they are easily and reliably measured and their variation with damage is clearly monotonic. Unfortunately, due to them being a global characteristic, frequencies offer a modest sensitivity to local damage, mainly when the damage intensity is limited [3]. As such, variations of temperature or humidity could cause changes in frequencies sometimes as large as those induced by damage.

With the increasing availability of more affordable experimental techniques, other modal quantities – modal shapes and modal curvatures – have been the focus of an increasing attention by researchers, with the aim of detecting low intensity damages.

In particular, modal curvatures are known to considerably change in the neighbourhood of the damage [4, 5]. However, their evaluation is not simple mainly for two reasons: (i) their variations due to distributed damage could spread over the entire structure [6]; (ii) in the presence of sharp damages, the evaluation of the modal curvature requires sensors placed in close proximity of the damage. For this

reason, this work starts with a critical review of the different approaches for damage identification, with a special focus on those using modal curvatures.

Making use of a perturbative solution of the equation of motion of a damaged beam, it is possible to obtain a closed form relationship between the modal curvature differences due to damage and the damage distribution itself [7]. Such a result, suggests that a proper filtering of the modal curvature variations must be carried out for using them in damage localization or in damage assessment techniques when used with other modal quantities, such as frequencies and mode shapes as shown in [8].

The validation of the procedure that makes use of the modal quantities measured by an experimental setup, able to record frequencies, modal shapes and modal curvatures, is performed by means of numerical investigation with pseudo-experimental data and of an experimental laboratory campaign.

The experiments deal with a free-free beam. Several damage cases are considered with different intensities. The contribution of using the modal curvature differences in the identification of damage position and intensity is evidenced.

2 MODAL CURVATURES

2.1 Filtering technique

In this section, we briefly review the main results in [6, 7] which concern the localization of damage through modal curvature. The transverse motion of a cracked beam is studied by exploiting the perturbative solution of the dynamic Euler-Bernoulli equation. The procedure is fully described in [6] and very shortly recalled here.

The dimensionless equation governing the i-th transverse mode of a damaged beam is:

$$\frac{d^4\phi_i(s)}{ds^4} - \varepsilon \frac{d^2}{ds^2}\left[\eta(s)\,\frac{d^2\phi_i(s)}{ds^2}\right] - \omega_i^2\phi_i^*(s) = 0 \tag{1}$$

where $s \in [0,1]$ is the dimensionless abscissa, $\phi(s)$ is the transverse displacement and $\eta(s)$ is a smooth function representing the damage shape, such that $\|\eta(s)\| = 1$. The eigenfunctions ϕ_i and eigenvalues ω_i^2 can be expanded as a power series in terms of the damage intensity ε ,i.e.,

$$\phi_i(x) = \widetilde{\phi}_i(x) - \varepsilon\,\overline{\phi}_i(x) + \mathrm{O}(\varepsilon^2), \qquad \omega_i^2 = \widetilde{\omega}_i^2 - \varepsilon\,\overline{\omega}_i^2 + \mathrm{O}(\varepsilon^2) \tag{2}$$

where $\widetilde{\phi}_i$ and $\widetilde{\omega}_i^2$ are respectively the ith eigenfunction and eigenvalue of the undamaged beam, and $\overline{v}_i$ and $\overline{\omega}_i^2$ are their first order variations. By taking into account only the contributions up to the first order in ε, the following system of ordinary differential equations is obtained

$$\text{0-}th\text{ order:} \qquad \frac{d^4\widetilde{\phi}_i(s)}{dx^4} - \widetilde{\omega}_i^2\widetilde{\phi}_i(s) = 0 \tag{3}$$

$$\text{1-}st\text{ order:} \qquad \frac{d^4\overline{\phi}_i(s)}{ds^4} - \widetilde{\omega}_i^2\overline{\phi}_i(s) = \overline{\lambda}_i\widetilde{\phi}_i(s) - \frac{d^2\eta_i(s)}{ds^2} \tag{4}$$

where the function $\eta_i(s)$ is the *modal damage shape* weighted through the ith modal curvature, *i.e.* $\eta_i(s) := \eta(s)\, d^2\overline{\phi}_i/ds^2$. Eq.(3) is simply the governing equation of the undamaged system.

The difference between the modal curvature of the damaged and undamaged beams, $\Delta\psi_k$, can be expressed in terms of the modal quantities of the undamaged system and the damage shape function $\eta(s)$ as in [6], i.e.,

$$\eta_k = -\Delta\psi_k + \frac{\Delta\omega_k^2}{\widetilde{\omega}_k^2}\frac{\widetilde{\psi}_k}{\|\widetilde{\psi}_k\|} + \sum_{l\neq k}\frac{\widetilde{\omega}_k^2}{\widetilde{\omega}_l^2}\int_0^1 \widetilde{\psi}_l^T(s)\Delta\psi_k(s)\mathrm{d}s\frac{\widetilde{\psi}_l}{\|\widetilde{\psi}_l\|^2}\,, \tag{5}$$

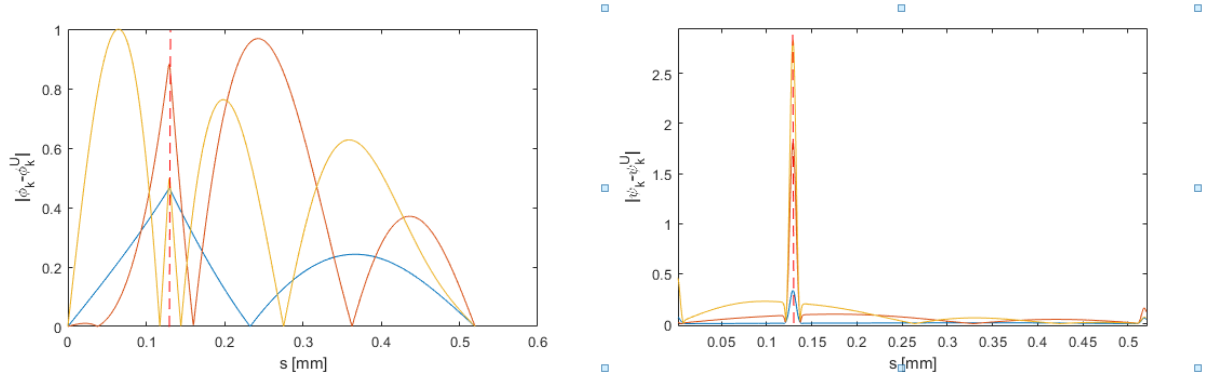

Figure 1: Modal displacement difference (left) between the damaged and undamaged system for the damage case D1 for the first three modes (blue - 1st mode; red - 2nd mode; yellow - 3rd mode). (right) Corresponding modal curvature differences. The dashed red line shows the actual position of the damage.

where $\Delta\omega_k^2 = \widetilde{\omega}_k^2 - \omega_k^2$ is the modal frequency variation, between the k-th modal frequency of the undamaged and damaged systems. For the sake of brevity, we have indicated the *k-th modal curvature*, i.e., the second derivative of the k-th mode shape, as $\psi_k(s) := \phi_k''(s)$.

Equation (5) highlights that the function χ_k, i.e., the product of the damage shape with the k-th modal curvature, is, as a matter of fact, the *observable quantity* of the inverse problem based on modal curvatures rather than the modal curvatures themselves. As such, if the damage occurs in a region where the k-th modal curvature vanishes, the damage shape can not be reconstructed from the k-th modal curvature. In addition, Eq. (5) shows that the damage shape can be evaluated only after the k-th modal curvature difference is filtered as that equation suggests; interestingly, all quantities that appear on the right hand side of the equation are indeed easy to measure: $\Delta\psi_k$ is the difference between the normalised k-th modal curvatures of the damaged and undamaged beam, $\Delta\omega_k^2$ is the difference of the corresponding modal frequencies, $\widetilde{\psi}_l$ is the l-th undamaged modal curvature divided by its norm $\|\widetilde{\psi}_l\|$.

2.2 Numerical evaluation of modal shapes and modal curvatures

In the case of sharp damages, modal curvatures are known to be localized quantities even if not properly filtered. In this respect Fig. 1a shows the first four mode displacement differences obtained by a numerical model of the free-free beam experimentally tested by the authors, whose mechanical and geometric characteristics are shown in Fig. 2 for damage cases D1 in Fig. 3. For the sake of comparison, Fig. 1b shows the corresponding modal curvature differences. It is seen from the figure that multiple peaks appear in the difference when considering modal displacements whereas a more localised information can be extracted from the modal curvature difference. In the case of mode shapes, these peaks are located in a region close to but not correspondent with the actual damage position (represented by a dashed red line). As already pointed out, such a circumstance makes the solely use of eigenmode difference in the damage localization problematic and potentially leading to false indications. However, their use in the objective function together with the eigenfrequencies variation can lead to a more accurate evaluation of the damage parameters with respect to the use of frequencies only.

2.3 Experimental evaluation of modal curvatures

Much care must be devoted when extracting modal curvatures from experimental data. When strain gauges are used to measure the structural response, the frequency response function measured at the

abscissa s_i for a point force applied at the abscissa s_j is

$$H_{ij}(\omega) = \frac{G_{ij}(\omega)}{G_{jj}(\omega)} \tag{6}$$

where $G_{jj}(\omega)$ is the auto-power spectral density of the input and $G_{ij}(\omega)$ is the cross-power spectral density between input and output. In particular, when strains are measured, Eq. (6) can be written as:

$$H_{ij}(\omega) = \sum_{k=1}^{\infty} \frac{\psi_k(x_i)\phi_k(x_j)/\rho L\omega^2||\phi_k||^2}{1-(\omega_k^2+i\eta_r\omega_k^2)/\omega^2}. \tag{7}$$

Differently from what happens when the response is measured in terms of accelerations, here, only an approximate normalization is obtainable. According to [9], for the purpose of normalization, it can be accepted that

$$\psi_k = -\omega_k \left(\frac{\rho}{EI}\right)^{1/2} \phi_k \tag{8}$$

which means that the hyperbolic terms have been neglected. With this assumption, the mass-normalized amplitude of the eigenfunctions at x_j can be derived from the numerator of the FRF where the forcing function is applied, that is:

$$\frac{\phi_k(x_j)}{\omega\sqrt{\rho L}||\phi_k||} = \left(\frac{U_{jjk}}{\omega_k}\left(\frac{EI}{\rho}\right)^{1/2}\right)^{1/2}. \tag{9}$$

When no strain gauge is available where the force is applied, the modal amplitude at x_j is calculated by taking the mean of the response at the two closest strain gauges, that is $U_{jjk} = (U_{(j-1)jk} + U_{(j+1)jk})/2$, which is used in Equation (9) to obtain the mass-normalized modal curvatures. Equations (7)-(9) are used to extract the curvature mode shapes from the results of the experimental tests.

The experiments were carried out at the laboratory of the Department of Structural and Geotechnical Engineering, Sapienza University of Rome, on a steel beam whose geometric and mechanical characteristics are reported in Fig. 2. The beam was dynamically excited by a point force generated by an electrodynamic shaker, that was driven by a white noise input signal up to a frequency of 2500/3000 Hz. To measure the proper frequency response function, the input force was recorded with a load cell installed at the base of the shaker stinger, which was realized with a thin steel bar with circular cross section. The response was measured using seven strain gauges equally spaced along the beam axis, in the damaged and undamaged cases. The results of the experimental campaign with the modal curvatures extracted through Eq. 9 are shown in Fig. 3-6.

In particular damage cases are reported in Figure 3. Case D1 includes a notch localized below the strain gauge #1 with a residual height of the damaged cross-section equal to $h^D = 3h/4$, case D2 has the same localization, but a residual height equal to $h^D = h/2$, case D3 the same damage as D2, plus a second notch of residual height $h^D = 3h/4$ located between strain gauges #5 and #6.

A reduction of natural frequencies with increasing damage is observed. This is shown by the shift of the peaks in Figure 4, which compares the modulus of the frequency response function in terms of strains in the undamaged and damaged (D2) cases. The frequency response function $H_{1P}(f)$ is measured in channel #1 for the forcing function applied at point P. The values of the first four natural frequencies are reported in Table 1 for the undamaged (U), and the three cases of damage under investigation (D1, D2, D3, Figure 3).

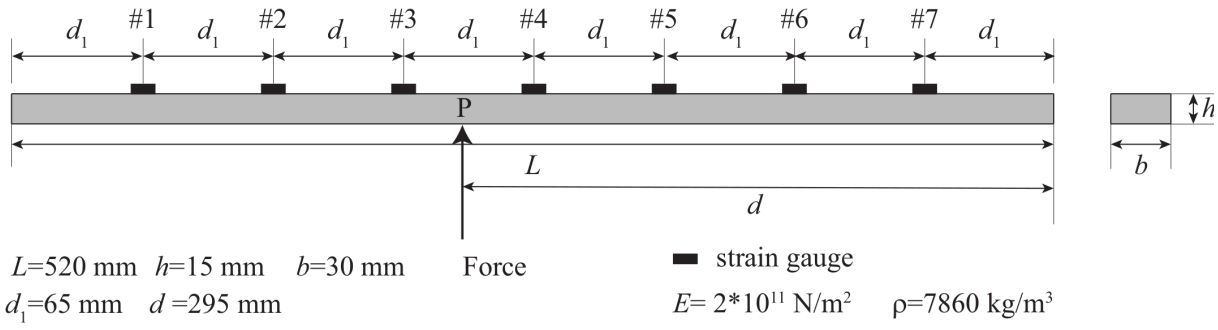

Figure 2: Geometry of the undamaged free-free (FF) beam and steel material properties.

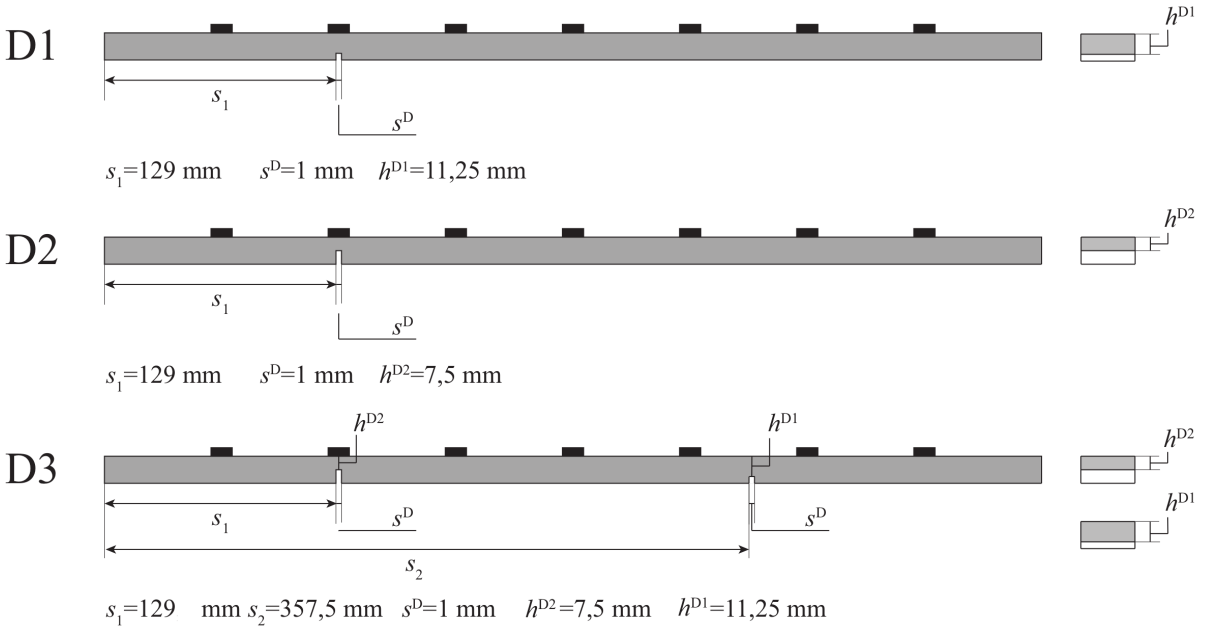

Figure 3: Damage cases for the steel free-free beam.

	f_1	f_2	f_3	f_4
U	293	808	1559	2546
D1	292	794	1539	2548
D2	284	744	1478	2535
D3	281	732	1470	2503

Table 1: Natural frequencies in the undamaged and damaged cases [Hz] - FF beam.

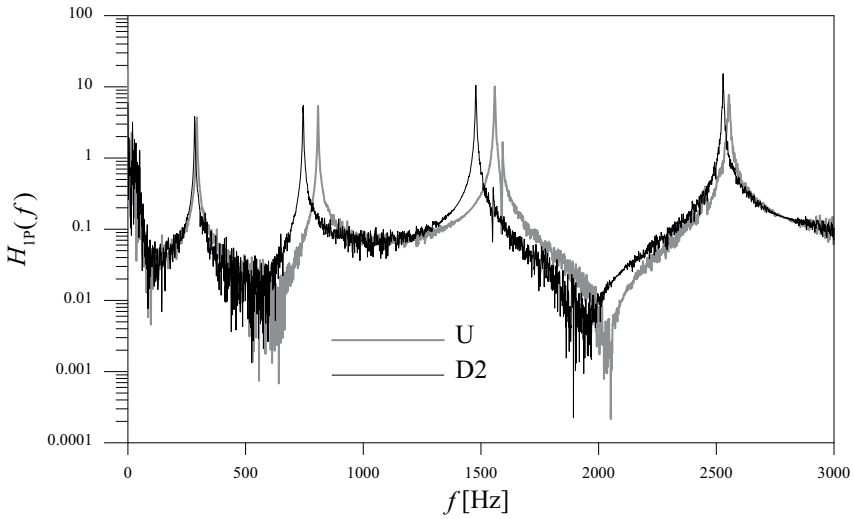

Figure 4: Component H_{1P} of the Frequency Response Function in terms of strains in the undamaged (U) and damaged (D2) cases.

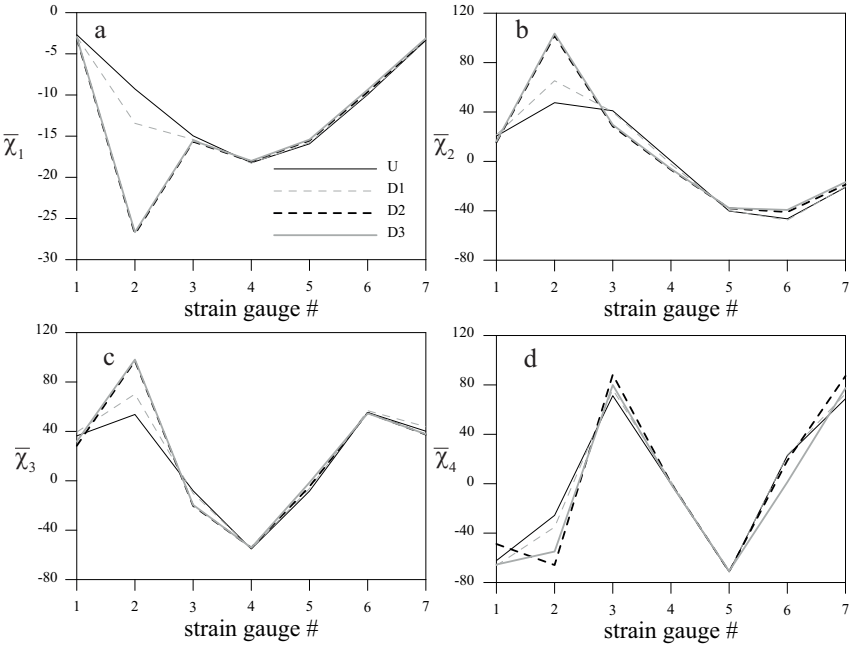

Figure 5: Experimental modal curvatures for the first (a), second (b), third (c), and fourth (d) modes in the undamaged and damaged cases.

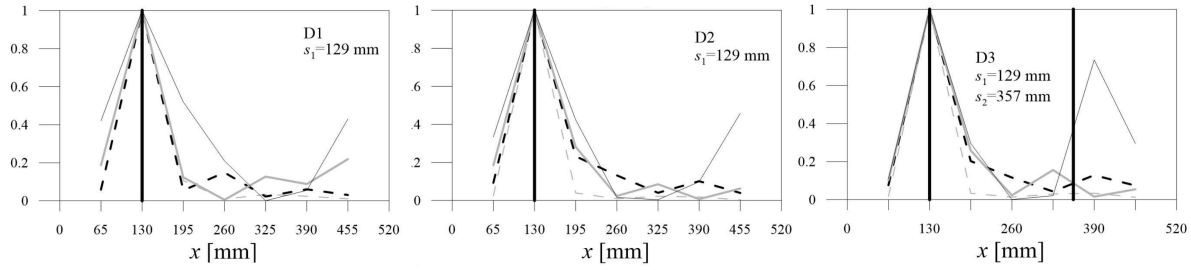

Figure 6: Curvature differences for the three damage states of the FF beam. Mode 1 - dashed grey line; Mode 2 - dashed black line; Mode 3 - grey thick line; Mode 4 - thin grey line.

Figure 5 shows the mass-normalized modal curvatures for the first four identified modes, in the undamaged and damaged states. For the sake of brevity we take

$$\overline{\psi}_k = \frac{\psi_k'' h}{2\sqrt{\rho L}||\phi_k||\kappa}\left(\frac{EI}{\rho}\right)^{1/4}. \tag{10}$$

Figure 6, which reports the variation of modal curvatures between the undamaged and damaged state, normalized so that the maximum equals one, shows that the local increase in curvature where damage is located is very clear when damage is placed just below strain gauge #2 (all cases). On the contrary, when damage is located between strain gauges #5 and #6 (D3), the presence of damage is less evident from the increase in curvature.

3 DAMAGE IDENTIFICATION

The analysis in previous paragraphs has shown that, in case of sharp damages, modal curvature can directly give information on the location of damage. However, the assessment of the damage intensity requires the definition of an inverse problem based on the comparison between the undamaged and damaged state responses. To do that, a finite element model of the beam in Fig. 2 is implemented in Ansys with n=520 B21 elements. The damage is schematically represented as a concentrated spring at position s with dimensionless intensity $k = \frac{2\ell}{h^U}\frac{1-\beta}{\beta}$ with $\beta = (EI^U - EI^D)/EI^U$, and EI^U and EI^D respectively the flexural rigidities of the undamaged and damaged cross sections [10]. An optimal estimate of the parameters k and s is obtained by minimizing an objective function which is built as the sum of differences between selected response quantities. As a first step, we consider an objective function which depends on the first m frequency differences, i.e.,

$$G_f(k,s) = \sum_{i=1}^{m}\left(\frac{\Delta\omega_i(k,s)}{\omega_i^U} - \frac{\Delta\omega_{ei}}{\omega_{ei}^U}\right)^2 \tag{11}$$

which is the sum of the squares of the differences between the numerical $\Delta\omega_i(k,s)$ and experimental $\Delta\omega_{ei}$ frequency variations between the undamaged and the damaged states, normalized with respect to the frequencies of the undamaged beam, ω_i^U and ω_{ei}^U. Since the $\Delta\omega_i(k,s)$ are not observable in closed-form, they are evaluated at discrete values of k and s, which enables to calculate the function (11) on a grid.

The $G_f(k,s)$ is shown in Fig. 7 by using three (m=3) and four (m=4) frequencies for the damage case D2. The insets in the figure show the corresponding values of the parameters s and k at the position of the

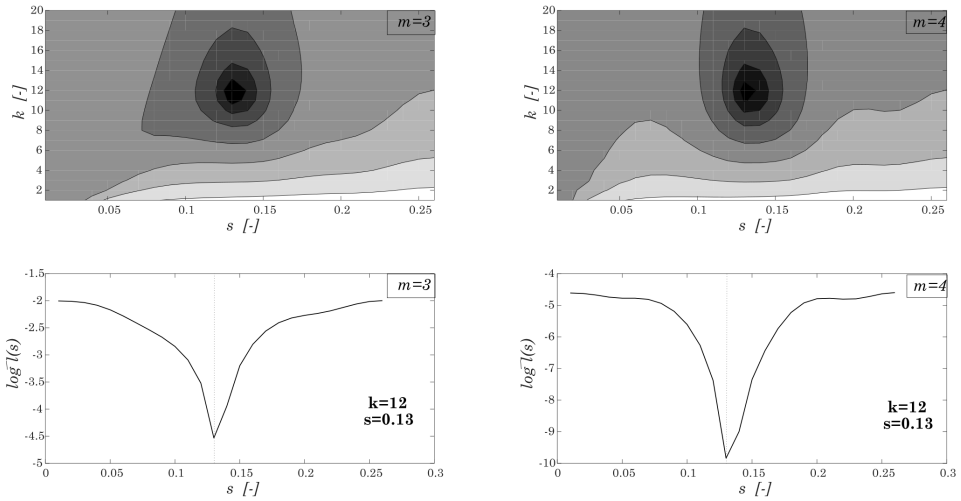

Figure 7: Objective function $G_f(k,s)$ calculated with three (left) and four (right) frequencies in the case of damage D2. The plots are the contour plot of the functional whereas the bottom plots are the curve obtained intersecting the functional with the plane $k = k_{min}$.

minimum, to be compared with the real position of the damage $\bar{s} = 0.129$ and equivalent stiffness of the damage $\bar{k} = 10$. These results show that already with three frequencies a good estimate of the damage position can be achieved despite having a 20% error on the damage intensity.

In order to verify the possible improvement of the identification using modal curvature differences, the following enhanced objective function is considered

$$G_{fc}(k,s) = G_f(k,s) + \alpha\, G_c(k,s) \tag{12}$$

where α is a positive scaling constant, assumed equal to 0.3 in the present case, and G_c is the function based on the modal curvature differences

$$G_c(k,s) = \sum_{i=1}^{n} \left(\frac{\Delta\psi_i(k,s)}{\|\psi_i^U\|} - \frac{\Delta\psi_{ei}}{\|\psi_{ei}^U\|} \right)^2 \tag{13}$$

with ψ_e the experimental modal curvatures. Since a robust localization of damage was already obtained with the first modal curvature difference (see Fig. 6), only the first modal curvature is included in the objective function ($n = 1$). The results in Fig. 8 show that the minimum of the enhanced G_{fc} is much sharper and the correct values of the parameter are obtained.

4 CONCLUSIONS

The great part of damage identification techniques used in the literature are based on the differences of the modal frequencies of the damaged and undamaged system. In this work, to enhance the solution of the inverse problem and to have a better estimate of damage parameters, we have examined the use of both modal displacements and modal curvatures. The latter have always been considered strictly related to the damage region but some drawbacks have been highlighted:

- modal curvature differences are influenced by the damage distribution in a more significant way than modal shape differences;

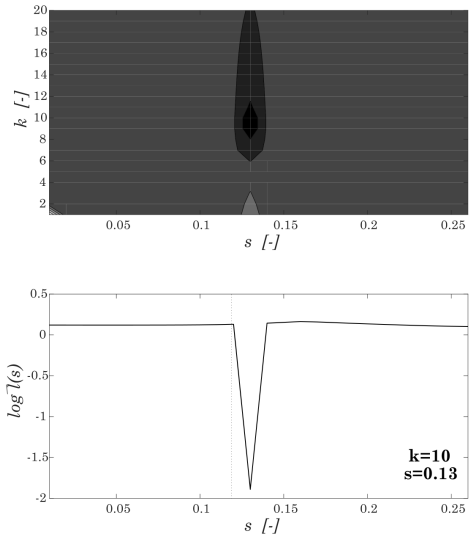

Figure 8: Objective function $G_{fc}(k,s)$ calculated with four frequencies and the first modal curvature difference in the case of damage D2. Contour plot of the function (top), plot of the curve obtained intersecting the functional with the plane $k = k_{min}$ (bottom).

- if the damage is extended compared to the characteristic dimensions of the structure, the use of modal curvatures in a damage identification technique requires them to be properly filtered;
- for sharp damages, modal curvature differences are also very sharp and this could make their experimental evaluation difficult.

With reference to an experimental campaign carried out on a free-free beam, we have shown the feasibility of using modal curvature variations, experimentally measured through strain gauges, together with modal frequency variations. For a certain damage scenario, we have compared the results of the identification obtained with an objective function weighing only the modal frequency differences and an enhanced function with both frequency and curvature variations. In the latter case, a more accurate estimate of the damage parameter was achieved and, in addition, the symmetric solution, which can not be distinguished by using only the modal frequency difference, was eliminated.

5 ACKNOWLEDGEMENTS

The support of Italian MIUR under the grant PRIN–2015, 2015TTJN95, P.I. Fabrizio Vestroni, "Identification and monitoring of complex structural systems" is gratefully acknowledged. The authors thank Giuseppe Marino for his support in carrying out the experiments.

References

[1] D Montalvao. A Review of Vibration-based Structural Health Monitoring with Special Emphasis on Composite Materials. *The Shock and Vibration Digest*, 38(4):295–324, jul 2006.

[2] Y F Fan, J Zhou, Z Q Hu, and T Zhu. Study on mechanical response of an old reinforced concrete arch bridge. *Struct. Control Hlth.*, 14(6):876–894, oct 2007.

[3] F Vestroni and D Capecchi. Damage detection in beam structures based on frequency measurements. *J. Eng. Mech.*, (126):761–768, 2000.

[4] A K Pandey, M Biswas, and M M Samman. Damage detection from changes in curvature mode shapes. *J. Sound Vib.*, 145(2):321–332, 1991.

[5] D Dessi and G Camerlengo. Damage identification techniques via modal curvature analysis: Overview and comparison. *Mech. Syst. Signal Pr.*, 52-53:181–205, feb 2015.

[6] J Ciambella and F Vestroni. The use of modal curvatures for damage localization in beam-type structures. *J. Sound Vib.*, 340:126–137, mar 2015.

[7] J. Ciambella, A. Pau, and F. Vestroni. Modal curvature-based damage localization in weakly damaged continuous beams. *Mechanical Systems and Signal Processing*, 121:171–182, apr 2019. ISSN 08883270. doi: 10.1016/j.ymssp.2018.11.012.

[8] D Capecchi, J Ciambella, A Pau, and F Vestroni. Damage identification in a parabolic arch by means of natural frequencies, modal shapes and curvatures. *Meccanica*, 51(11):2847–2859, nov 2016.

[9] F.L.M. Dos Santos, B. Peeters, J. Lau, W. Desmet, and L.C.S. Goes. An overview of experimental strain-based modal analysis methods. In *Proceedings of ISMA 2014 - International Conference on Noise and Vibration Engineering and USD 2014 - International Conference on Uncertainty in Structural Dynamics*, pages 2453–2468, 2014.

[10] A. Pau, A. Greco, and F. Vestroni. Numerical and experimental detection of concentrated damage in a parabolic arch by measured frequency variations. *JVC/Journal of Vibration and Control*, 17 (4):605–614, 2011. doi: 10.1177/1077546310362861. cited By 38.